

1 **Parallel genetic changes underlie integrated craniofacial traits in an adaptive radiation of**  
2 **trophic specialist pupfishes**

3

4 Michelle E. St. John<sup>1,2</sup>, Julia C. Dunker<sup>1</sup>, Emilie J. Richards<sup>1,2</sup>, Stephanie Romero<sup>3</sup>, Christopher  
5 H. Martin<sup>1,2</sup>

6

7 <sup>1</sup>Department of Integrative Biology, University of California, Berkeley, CA 94720

8 <sup>2</sup>Museum of Vertebrate Zoology, University of California, Berkeley, CA 94720

9 <sup>3</sup>Department of Evolution and Ecology, University of California, Davis, CA 95616

10

11

12 Keywords: quantitative trait loci, ecological speciation, functional morphology, ecomorph,

13 lepidophagy, durophagy

14 Correspondence: [chmartin@berkeley.edu](mailto:chmartin@berkeley.edu)

15

16 **Abstract**

17 Many factors such as divergence time, shared standing genetic variation, frequency of  
18 introgression, and mutation rates can influence the likelihood of whether populations adapt to  
19 similar environments via parallel or non-parallel genetic changes. However, the frequency of  
20 parallel vs non-parallel genetic changes resulting in parallel phenotypic evolution is still  
21 unknown. In this study, we used a QTL mapping approach to investigate the genetic basis of  
22 highly divergent craniofacial traits between scale- and snail-eating trophic specialist species  
23 across similar hypersaline lake environments in an adaptive radiation of pupfishes endemic to  
24 San Salvador Island, Bahamas. We raised F2 intercrosses of scale- and snail-eaters from two  
25 different lake populations of sympatric specialists, estimated linkage maps, scanned for  
26 significant QTL for 30 skeletal and craniofacial traits, and compared the location of QTL  
27 between lakes to quantify parallel and non-parallel genetic changes. We found strong support for  
28 parallel genetic changes in both lakes for five traits in which we detected a significant QTL in at  
29 least one lake. However, many of these shared QTL affected different, but highly correlated  
30 craniofacial traits in each lake, suggesting that pleiotropy and trait integration should not be  
31 neglected when estimating rates of parallel evolution. We further observed a 23-52% increase in  
32 adaptive introgression within shared QTL, suggesting that introgression may be important for  
33 parallel evolution. Overall, our results suggest that the same genomic regions contribute to  
34 parallel integrated craniofacial phenotypes across lakes. We also highlight the need for more  
35 expansive searches for shared QTL when testing for parallel evolution.

36

37

38

## 39 **Introduction**

40 Convergent evolution describes the independent evolution of similar phenotypes in response to  
41 similar selective pressures and provides strong support for ecological adaptation (Losos 2009;  
42 Schluter 2000). This includes both non-parallel genetic changes, such as the evolution of  
43 antifreeze glycoproteins in icefishes or the ‘thunniform’ body shape of lamnid sharks and tunas  
44 (Chen et al. 1997; Donley et al. 2004), and parallel genetic changes such as tetrodotoxin  
45 resistance in snakes and pufferfishes or the evolution of voltage-gated sodium channels in  
46 mormyrid and gymnotiform electric fishes (Hopkins 1995; Katz 2006; Jost et al. 2008; Feldman  
47 et al. 2009; Zakon et al. 2006). Instances of convergence across independent lineages (i.e., across  
48 groups that lack a recent common ancestor and shared genetic backgrounds) provide the  
49 strongest evidence for adaptation; however, repeated evolution of similar phenotypes in response  
50 to similar selective pressures among lineages derived from the same ancestral population can  
51 also provide insight into the process of adaptation. Understanding this process, traditionally  
52 known as parallel evolution (Futuyma 1986), is important because it can help to tease apart the  
53 contributions of natural selection and shared genetic constraints to similar phenotypes (Schluter  
54 et al. 2004; Stuart et al. 2017). Parallel phenotypic evolution can also occur via parallel or non-  
55 parallel genetic changes (e.g., Cresko et al. 2004), but even non-parallel genetic changes  
56 occurring in the same ancestral genetic background (e.g. Chan et al. 2010; Xie et al. 2019)  
57 provide weaker evidence for adaptation than convergence across independent lineages due this  
58 shared history. Despite substantial attention, the frequency and likelihood of parallel phenotypic  
59 evolution via parallel or non-parallel genetic changes is still relatively unknown (Stern and  
60 Orgogozo 2008; Stern 2013; Rosenblum et al. 2014).

61           Many factors influence whether parallel phenotypic evolution in similar environments is  
62 produced by parallel or non-parallel genetic mechanisms. First, recently diverged species exhibit  
63 increased probabilities of genetic parallelism when adapting to similar environments. Recently  
64 diverged taxa may inhabit similar environments more frequently or they may have similar  
65 genetic architectures, similar genetic variance-covariance matrices, or similar genetic  
66 backgrounds that produce similar epistatic interactions (Conte et al. 2012; Rosenblum et al.  
67 2014). Second, any mechanism that allows the use of the same adaptive genetic mechanism  
68 should increase the likelihood of convergence via parallelism, including the availability of shared  
69 standing genetic variation and introgression (Rosenblum et al. 2014). For example, threespine  
70 sticklebacks colonized freshwater thousands of times and converged on similar phenotypes  
71 largely due to selection on an ancient shared pool of marine standing genetic variation (Jones et  
72 al. 2012; Feulner et al. 2013; Nelson and Cresko 2018; Haenel et al. 2019; but see: Chan et al.  
73 2010; Stuart et al. 2017). Similarly, increased adaptive introgression should also make genetic  
74 parallelism more likely (Grant et al. 2004; Morjan and Rieseberg 2004; Hedrick 2013; Taylor et  
75 al. 2020). Third, adaptive genetic variation with larger effect sizes and fewer pleiotropic effects  
76 should be reused more frequently across populations, particularly when a population is far from a  
77 new adaptive optimum (Linnen et al., 2013; Orr, 2005; Stern, 2013). Finally, de novo mutations,  
78 large mutational target sizes, and polygenic adaptive phenotypes are more likely to result in  
79 parallel phenotypic evolution via non-parallel genetic pathways (Wittkopp et al. 2003; Kowalko  
80 et al. 2013; Bolnick et al. 2018, but see: Colosimo et al. 2004; Chan et al. 2010; Xie et al. 2019).

81           Quantitative trait locus (QTL) mapping is often used to infer whether parallel or non-  
82 parallel genetic changes underlie parallel phenotypes. However, many QTL studies only  
83 investigate a limited number of traits that are controlled by large effect loci, which may bias the

84 literature towards supporting genetic parallelism (Conte et al. 2012). This bias may be  
85 exacerbated by the fact that in many QTL studies the genomic regions associated with a parallel  
86 phenotype are large, contain many genes, and their effects on phenotypic variance are  
87 overestimated in under-powered studies (Beavis 1998). These methodological and experimental  
88 limitations reduce confidence in the specific genomic regions associated with a parallel  
89 phenotype and, by extension, reduce confidence in whether parallel evolution was due to parallel  
90 or non-parallel genetic changes. One possible solution is to compare the genomic regions  
91 associated with many different phenotypes across populations (Erickson et al. 2016). In this  
92 scenario, shared genomic regions across populations provide strong support for genetic  
93 parallelism, except in the likely rare instances of independent de novo mutations within the same  
94 region (O’Brown et al. 2015; Xie et al. 2019; Chan et al. 2010).

95         The San Salvador Island (SSI), Bahamas pupfish radiation is an excellent system for  
96 investigating the genetic underpinnings of parallel ecomorph phenotypes because novel trophic  
97 specialists occur in sympatry across multiple hypersaline lake populations on the island. The  
98 radiation includes three pupfish species: a generalist pupfish (*Cyprinodon variegatus*), a scale-  
99 eating (lepidophagous) pupfish (*C. desquamator*), and a snail-eating (durophagous) pupfish (*C.*  
100 *brontotheroides*; Martin and Wainwright 2013). The snail- and scale-eating pupfishes are  
101 endemic to SSI and occur in sympatry with one another and the generalist pupfish.

102         Among lakes, specialists have converged on multivariate phenotypes that are adaptive for  
103 their given ecological niche. For example, scale-eaters across all lakes exhibit increased oral jaw  
104 size (Martin & Wainwright, 2013; Hernandez et al. 2018) and reduced lower jaw angles during  
105 scale-eating strikes which may play a critical role in scale-biting performance during high-speed  
106 strikes on their prey (St. John et al. 2020b). Similarly, the snail-eating pupfish exhibits a novel

107 nasal protrusion which may improve oral snail-shelling performance or result from sexual  
108 selection (Martin and Wainwright 2013; St. John et al. 2020a). Furthermore, the nasal protrusion  
109 of the snail-eating species varies substantially among lake populations (Martin and Feinstein  
110 2014; Hernandez et al. 2018). Despite the importance of these species characteristics, we still do  
111 not understand how their genetic architecture varies across populations.

112         There is some evidence to suggest that parallel genetic changes underlie specialist  
113 phenotypes on SSI. First, the SSI radiation is very young, diverging only about 10 kya (Hagey  
114 and Mylroie 1995). Second, previous genomic analyses show that many of the alleles associated  
115 with trophic specialization arrived on SSI from Caribbean-wide standing genetic variation within  
116 generalist pupfish populations, but there are also some de novo adaptive mutations associated  
117 with scale-eating (Richards et al. 2021). Scale-eaters form a monophyletic group, suggesting a  
118 shared genetic component to the scale-eating phenotype across lakes (Richards and Martin  
119 2017). In contrast, snail-eaters and generalists often genetically cluster together by lake instead  
120 of by species—suggesting that non-parallel genetic changes could underlie parallel snail-eater  
121 phenotypes across lakes (Martin and Feinstein 2014; Richards and Martin 2017). Furthermore,  
122 previous studies have documented strong genetic divergence between scale-eaters from Crescent  
123 Pond and all other populations of scale-eater (Richards & Martin, 2017; Richards et al., 2021).

124         In this study we mapped the genetic basis of 30 skeletal craniofacial and body traits  
125 associated with snail- and scale-eating using lab-reared F2 intercrosses from Crescent Pond and  
126 Little Lake. We called variants, estimated linkage maps, and performed QTL analyses  
127 independently for each F2 population. We found that only one trait—cranial height—mapped to  
128 the same genomic region in both Crescent Pond and Little Lake, but 4 of the 5 remaining  
129 significant QTL detected in one lake mapped to the same genomic region as a highly correlated

130 craniofacial trait in the second lake. Ultimately, we conclude that parallel evolution through  
131 reuse of introgressed adaptive alleles is acting to produce similar snail- and scale-eating  
132 phenotypes across lake populations on SSI.

133

## 134 **Methods**

### 135 **Genetic cross**

136 Currently, pupfish species can be found in 12 hypersaline lakes across the island: generalist  
137 pupfish are found in allopatry in five lakes, the generalist and snail-eating pupfish are found in  
138 sympatry without the scale-eater in two lakes, the generalist and scale-eater are found in  
139 sympatry in a single lake, and all three species are found in sympatry in four lakes (Martin and  
140 Feinstein 2014). We collected wild-caught scale-eating and snail-eating pupfishes from two  
141 different sympatric populations (containing all three species) on SSI – Crescent Pond and Little  
142 Lake—during the years of 2011 and 2013-2015 using seine nets. We brought individuals back to  
143 the University of California, Davis or the University of California, Berkeley and a single wild-  
144 caught scale-eating female from each lake was allowed to breed freely with a single wild-caught  
145 snail-eating male from the same lake resulting in two separate genetic crosses (one cross from  
146 Crescent Pond and one cross from Little Lake). At least four F1 offspring from each hybrid  
147 population were crossed to produce F2 intercrosses, resulting in 354 individuals from Crescent  
148 Pond and 287 individuals from Little Lake included in this study. All fish were maintained in 40-  
149 L tanks at 5-10ppt salinity at the University of California, Davis or the University of California,  
150 Berkeley. We fed fry a diet of newly hatched *Artemia* nauplii for approximately 40 days post  
151 fertilization, after which they were switched to the adult diet of frozen and pellet foods. We  
152 euthanized fish in an overdose of MS-222 (Finquel, Inc.) according to the approved University of

153 California, Davis Institutional Animal Care and Use Protocol #17455 or University of California,  
154 Berkeley IACUC Protocol AUP-2015-01-7053, and stored them in 95% ethanol.

155

## 156 **Phenotyping**

### 157 **Sex and Mate Preferences**

158 For individuals from Crescent Pond, we recorded their sex using their sexually dimorphic body  
159 and fin coloration. Male pupfish develop a blue iridescent coloration along their anteriodorsal  
160 surface and a black marginal band along their caudal fin (Echelle and Echelle 2020).

161       Once F2 hybrids reached sexual maturity, we performed mating assays using a subset of  
162 the hybrid females from Crescent Pond to estimate mate preferences for snail- or scale-eating  
163 mates (N=74). Prior to the mating assays, female fish were isolated for at least twelve hours and  
164 conditioned on frozen bloodworms with a 12:12 light:dark cycle. Mating assays occurred in three  
165 1.1 m diameter kiddie pools (5-10ppt salinity). Pools were covered with gravel substrate and  
166 divided in half. In each half, we placed three clear plastic 7.5-L Kritter Keepers in a row  
167 containing three conspecific males housed individually to avoid aggression. Size-matched scale-  
168 eater males were placed on one side of each arena and snail-eating males on the other. Once the  
169 males were placed in individually in clear boxes, a female F2 hybrid from Crescent Pond was  
170 placed into the center of one of the three kiddie pools, chosen at random. We considered females  
171 acclimated to the pool once they had visited both rows of males, after which we started the  
172 seven-minute trial period. During each trial we recorded the amount of time a female spent  
173 within one body-length of each species. Each female was tested consecutively in all three pools,  
174 and we used the mean of her association time (scale-eater association time / total association

175 time during each 7-minute trial) across all three pools for QTL analysis. Size-matched males  
176 were periodically rotated into and among kiddie pools during the 12-month testing period.

177

## 178 **Morphological Traits**

179 To measure skeletal phenotypes in our F2 intercrosses, we cleared and double-stained each  
180 specimen with alizarin red and alcian blue. Before clearing and staining, each fish was skinned  
181 and fixed in 95% ethanol. We then fixed specimens in 10% buffered formalin for at least one  
182 week and stained batches of individually labeled specimens following Dingerkus and Uhler's  
183 (1977) protocol. We suspended cleared and stained specimens in glycerin, and photographed  
184 their left lateral side using a Canon EOS 60D digital SLR camera with a 60 mm macro lens. For  
185 each individual, we took two types of photographs: first, we took a whole-body photograph to  
186 calculate fin and body measurements and second, a lateral skull image to calculate craniofacial  
187 measurements (Figure 1). We used DLTdv8 software (Hedrick 2008) to digitize 11 landmarks  
188 on each whole body image and 19 landmarks on each lateral skull image following the  
189 morphometric methods described in Martin et al. (2017). For individuals from Crescent Pond, we  
190 also weighed the adductor mandibulae muscle mass. Each image included a standardized grid  
191 background which we used to calibrate and transform our measurements from pixels into  
192 millimeters. In total, we measured 354 individuals from Crescent Pond and 287 individuals from  
193 Little Lake. We used R to convert the 30 landmarks into linear distances. To reduce  
194 measurement error due to the lateral positioning of the specimens, we took the mean distances  
195 from the two clearest skull and whole-body photographs for each individual when possible. If an  
196 individual did not have two clear photographs for each orientation, we measured the single  
197 clearest photograph. Finally, we size-corrected each trait by using the residuals from a linear

198 model including the log-transformed measurement of each trait as the response variable and log-  
199 transformed standard length as the predictor variable. We investigated whether size-corrected  
200 traits varied between the two populations using a PCA and a MANOVA test, but found no  
201 appreciable difference between them (Fig. S1, num df = 28, approximate  $F$ -value= 0.34,  $P = 1$ )

202

### 203 **Genotyping**

204 We genotyped individuals using three different methods: First, we used whole genome  
205 resequencing for the wild-caught F0 parental generation of our Crescent Pond and Little Lake  
206 intercrosses. We used DNeasy Blood and Tissue Kits (Qiagen, Inc.) to extract DNA from the  
207 muscle tissue of each fish and quantified it on a Qubit 3.0 fluorometer (ThermoFisher Scientific,  
208 Inc.). Genomic libraries were then prepared at the Vincent J. Coates Genomic Sequencing Center  
209 (QB3) using the automated Apollo 324 system (WaterGen Biosystems, Inc.). Samples were  
210 fragmented using Covaris sonication and barcoded with Illumina indices. A quality check was  
211 also performed on all samples using a Fragment Analyzer (Advanced Analytical Technologies,  
212 Inc.). We used 150 paired-end sequencing on an Illumina HiSeq4000 for these four parental  
213 samples along with an additional 38 samples that were included in a previous study (Richards  
214 and Martin 2017).

215         Second, in addition to the 190 previously sequenced individuals from Crescent Pond used  
216 for a QTL mapping study (Martin et al. 2017), we included an additional 164 F2 individuals  
217 from Crescent Pond sequenced using double-digest restriction site associated sequencing  
218 (ddRADseq) following similar library prep and sequencing methods described in Martin et al.  
219 (2015, 2016, 2017). Briefly, we prepared four indexed libraries each containing 96 barcoded

220 individuals. We sequenced these using 100 single-end high-output mode on two lanes of  
221 Illumina Hiseq4000 at the Vincent J. Coates Genomic Sequencing Center (QB3).

222 Finally, we sequenced all F2 individuals from Little Lake and a subset of previously  
223 sequenced, but low-coverage Crescent Pond F2's (N=84), using Nextera-tagmented reductively-  
224 amplified DNA (NextRad) sequencing (Russello et al. 2015). We followed the above methods  
225 for DNA extraction and sent samples to SNPsaurus (SNPsaurus, LLC) for quality checking,  
226 NextRad library preparation, and 150 single-end sequencing on two lanes of Illumina Hiseq4000  
227 at the University of Oregon sequencing core.

228

## 229 **Calling Variants**

230 We used the following methods to call variants separately for: 1) the Crescent Pond intercross (2  
231 parents and 354 F2 hybrids), and 2) the Little Lake intercross (2 parents and 285 F2 hybrids):  
232 First, we inspected raw read quality using FastQC (Babraham Bioinformatics Institute, v0.11.7)  
233 and trimmed reads to their appropriate length (100bp for samples sequenced with ddRAD, and  
234 150bp for samples sequenced with NextRAD) using TrimGalore! (v0.6.4). For samples that were  
235 sequenced using both ddRAD and NextRad methods, we concatenated trimmed raw reads into a  
236 single file. We next used bwa-mem to map reads from all individuals in an intercross, both  
237 parents and offspring, to the *Cyprinodon brontotheroides* reference genome (v 1.0; total  
238 sequence length = 1,162,855,435 bp; number of scaffolds = 15,698, scaffold N50 = 32 Mbp;  
239 (Richards et al. 2021)). We identified duplicate reads using MarkDuplicates and created BAM  
240 indices using BuildBamIndex in the Picard package ([http://picard.sourceforge.net\(v.2.0.1\)](http://picard.sourceforge.net(v.2.0.1))).  
241 Following the best practices guide from the Genome Analysis Toolkit (v 3.5; (Depristo et al.  
242 2011)), we called and refined our single nucleotide polymorphism (SNP) variant data set using

243 the program HaplotypeCaller. Pupfish lack high-quality known alleles because they are a non-  
244 model organism; we therefore used the recommended hard filter criteria (QD < 2.0; FS < 60;  
245 MQRankSum < -12.5; ReadPosRankSum < -8; (Depristo et al. 2011; Marsden et al. 2014)) to  
246 filter our SNP variant dataset. Ultimately, we detected 13.7 million variants in our Crescent Pond  
247 dataset and 14.4 million variants in our Little Lake dataset.

248 We used the program STACKS to further filter our dataset and convert our vcf files into  
249 phenotype and genotype comma-separated values files that could be imported into the Rqtl  
250 program. Specifically, we used the populations program to filter out variants that were not  
251 present in both the parental and F2 populations, and to filter out variants found in 10% or less of  
252 the population. From this filtering step we retained 36,318 variants with 46.5 mean mappable  
253 progeny per site in Crescent Pond and 87,579 variants with 85.984 mean mappable progeny per  
254 site in Little Lake.

255 We continued to filter our datasets using the Rqtl (v1.46-2), and ASMap (v1.0-4)  
256 packages (Broman et al. 2003; Taylor and Butler 2017). We started filtering by removing  
257 individuals that did not contain any filtered variants and any duplicate individuals. This reduced  
258 our Crescent Pond data set to 227 individuals, and our Little Lake data set to 281 individuals.  
259 Next, we filtered markers that had >0.98 or <0.1 heterozygosity (Crescent Pond: markers  
260 =15,247, Little Lake: markers=14,661). This step also filtered out 13 individuals from Crescent  
261 Pond which only contained markers with >0.98 or <0.1 heterozygosity. Before constructing our  
262 genetic maps, we set aside markers that appeared to suffer from segregation distortion. We used  
263 the pullCross() function from the ASmap package to set aside markers in both data sets that were  
264 missing in >75% of individuals, departed from Mendelian ratios (1:2:1), or any co-located  
265 markers for the initial construction of the linkage maps. This filtering retained more than twice

266 the number of markers for Crescent Pond than Little Lake. We therefore used a stricter filtering  
267 threshold for missing data (i.e., removing markers with >72% missing data) for our Crescent  
268 Pond dataset to construct linkage maps of comparable sizes for downstream comparative  
269 analyses. At the end of this filtering process the Crescent Pond dataset contained 214 individuals  
270 and 657 markers and the Little Lake dataset contained 281 individuals with 490 markers.

271

### 272 **Linkage Map Construction**

273 We used the `mstmap.cross()` function to form initial linkage groups and order markers, using the  
274 kosambi method for calculating genetic distances and a clustering threshold of  $P = 1 \times 10^{-14}$  for  
275 Little Lake and  $P = 1 \times 10^{-20}$  for Crescent Pond. After forming these initial linkage groups, we  
276 used the `pushCross()` function from the `ASmap` package to integrate previously set aside markers  
277 back into our map. We pushed markers back based on a segregation ratio of 3:4:3 and we pushed  
278 back any markers that had previously been designated as co-located. This increased our map  
279 sizes to 817 markers for Crescent Pond and 580 markers for Little Lake. With these additional  
280 markers, we re-estimated our linkage map using the `est.rf()` and `formLinkageGroups()` functions  
281 from the `Rqtl` package. We used a max recombination fraction of 0.35 and a minimum LOD  
282 threshold of 5 to estimate linkage groups for both data sets. We used the  
283 `droponemarker()` command from `Rqtl` with an error probability of 0.01 to identify and drop  
284 problematic markers from the genetic maps, including dropping linkage groups with 3 or fewer  
285 markers. Finally, we visually inspected our linkage groups using `plotRF()` from the `Rqtl` package,  
286 and merged linkage groups which had been incorrectly split up using the `mergeCross()` function  
287 from the `ASmap` package. Ultimately our final genetic maps included: 1) Crescent Pond: 214

288 individuals, 743 markers, 24 linkage groups and 2) Little Lake: 281 individuals, 540 markers,  
289 and 24 linkage groups (**Figure 2**).

290

## 291 **QTL Analyses**

292 We mapped QTL for 29 skeletal traits for both populations, and additional morphological  
293 (adductor mandibulae muscle mass) and behavioral traits (mate preference) for Crescent Pond.  
294 We used the Rqtl2 package (v0.22-11) to calculate genotype probabilities with a multipoint  
295 hidden Markov model using an error probability of 0.0001 and a Kosambi map function. We  
296 calculated kinship matrices to account for the relationship among individuals in two ways: 1)  
297 overall kinship, which represents the proportion of shared alleles between individuals, and 2)  
298 kinship calculated using the leave-one-chromosome-out method (LOCO). We used the scan1()  
299 function to perform three separate genome scans using a single-qt1 model by: 1) Haley-Knott  
300 regression, 2) a linear mixed model using the overall kinship matrix, and 3) a linear mixed model  
301 using the LOCO kinship matrix. For our Crescent Pond data set we also included sex as an  
302 additive covariate. We assessed the significance of all three models using two significance  
303 thresholds  $P < 0.1$  and 0.05 based on 1000 permutations each, using the scan1perm() function.  
304 As noted above the scan1() function can use several different methods to determine if a region is  
305 significantly associated with a given phenotype (Broman et al., 2019; Haley & Knott, 1992;  
306 Yang, Zaitlen, Goddard, Visscher, & Price, 2014; Yu et al., 2006), however, it is clear from  
307 previous theoretical work that many of these methods may suffer from type II error depending on  
308 the size of an organism's genome, the density of markers in a linkage map, or the complexity of  
309 the phenotypic traits being measured (Lander and Botstein 1989; Risch 1990). We therefore  
310 relaxed the  $P$ -value cut off from 0.05 to 0.1 to capture potentially important genomic regions.

311 This relaxation is further supported by the LOD scores associated with regions significant at the  
312  $P < 0.1$  level because they all exceed the traditional threshold of 3 (Nyholt 2000), the more  
313 conservative threshold of  $\sim 3.3$  (Lander and Kruglyak 1995; Nyholt 2000), the suggestive  
314 threshold of 1.86 (Lander and Kruglyak 1995), and are in line with estimates of significant LOD  
315 thresholds in previous studies (Erickson et al. 2016). All three of these methods detected similar  
316 QTLs and moving forward we only used the Haley-Knott regression method.

317 For each trait, we calculated the location of the maximum LOD score, and used the `fit1()`  
318 function to re-fit a single-QTL model at this location. We used the newly calculated LOD score  
319 to estimate the proportion of variance explained by the QTL and to calculate a  $P$ -value  
320 associated with each significant QTL ( $\chi^2$ -test). We also used the location of the maximum LOD  
321 score to calculate 95% Bayes credible intervals using the `bayes_int()` function from the `Rqtl2`  
322 package. We note that the maximum LOD score associated with every trait across both ponds  
323 exceeded the suggestive threshold of 1.86 (Lander and Kruglyak 1995). We used the  
324 `find.markerpos()` function from `Rqtl` to determine where markers in each linkage map fell within  
325 the reference genome. With this information we were able to determine the scaffolds/positions  
326 from the reference genome that fell within the 95% credible intervals for each putative QTL.  
327 Finally, we used the `maxmarg()` function from the `Rqtl2` package to find the genotype with the  
328 maximum marginal probability at the location of the maximum LOD. We used these genotypes  
329 to visualize the relationship between genotype and phenotypes.

330

### 331 **Identifying adaptive alleles within QTL regions**

332 For each scaffold that fell within a QTL's credible interval we calculated the minimum and  
333 maximum position for that scaffold (that was identified in the putative QTL region) and searched

334 the *C. brontotheroides* reference genome for annotated genes within the region. We then  
335 compared this list to a previously published list of genes that 1) contained or were adjacent to  
336 (within 20 kbp) fixed or nearly fixed ( $F_{st} > 0.95$ ) SNPs between specialist species on SSI, and 2)  
337 showed significant evidence of a hard selective sweep in both the site frequency spectrum-based  
338 method SweeD (Pavlidis et al. 2013) and the linkage-disequilibrium-based method OmegaPlus  
339 (Alachiotis et al. 2012). We hereafter refer to these loci as adaptive alleles. We also noted  
340 whether adaptive alleles within QTL regions were classified as de novo, introgressed, or as  
341 standing genetic variation on SSI (Richards et al. 2021). We used a bootstrap resampling method  
342 to determine whether the observed proportions of adaptive alleles originating from de novo,  
343 introgression, or standing genetic variation found within QTL 95% credible intervals were  
344 different than the proportions expected when drawn from the genome at random. We used the  
345 boot (v. 1.3-25) package (Buckland et al. 1998; Canty and Ripley 2021) to resample our entire  
346 adaptive allele dataset (with replacement) 10,000 times. We then used the boot.ci() command  
347 from the boot package to calculate the 95% credible intervals around expected proportions of de  
348 novo, introgressed, and standing adaptive alleles. We performed these calculations separately for  
349 scale-eater and snail-eater adaptive alleles.

350

## 351 **Results**

### 352 **Linkage Map Construction**

353 We identified 24 linkage groups from 743 markers for Crescent Pond, and 24 linkage groups  
354 from 540 markers for Little Lake (**Figure 2**). Previous karyotypes of *Cyprinodon* species  
355 estimated 24 diploid chromosomes, matching the linkage groups in this study (Liu & Echelle,  
356 2013; Stevenson, 1981). The total map length for Crescent Pond was 7335 cM and the total map

357 length for Little Lake was 5330; the largest linkage groups for each map were 740 cM and 380  
358 cM, respectively, and inter-marker map distance did not exceed 20cM in either map. To compare  
359 our maps and to determine if the same genomic regions were being reused across lakes, we  
360 identified where each marker was located in our reference genome. Overall, we found 324  
361 markers in both maps that were within 10 Kbp of one another, indicating that 60% of the Little  
362 Lake map was also present in the Crescent Pond map and 44% of the Crescent Pond map was  
363 present in the Little Lake map (**Figure 3**).

364

### 365 **Craniofacial QTL**

366 We detected three significant QTL in Crescent Pond and five QTL in Little Lake (**Table 1**,  
367 **Table 2**). In Crescent Pond, we identified QTL associated with the depth of the dentigerous arm  
368 of the premaxilla, cranial height, and adductor mandibulae muscle mass. Cranial height in  
369 Crescent Pond mapped to linkage group (LG) 10. Dentigerous arm depth and adductor  
370 mandibulae muscle mass both mapped to LG 13, which also contained the max LOD scores for  
371 two additional jaw traits (jaw opening in-lever and maxillary head height; **Table 2**). The 95%  
372 credible intervals for all these traits overlapped, suggesting that LG 13 may contain a single  
373 pleiotropic locus or many loci that affect all four traits.

374 In Little Lake, we detected significant QTL associated with jaw closing in-lever (i.e.  
375 height of the coronoid process on the articular: LG9), width and depth of the dentigerous arm of  
376 the premaxilla (LG3 and LG6), maxillary head protrusion (LG10), and cranial height (LG1;  
377 **Table 1, Table 2**). The 95% credible interval for dentigerous arm width on LG3 also contained  
378 the max LOD score for lower jaw length, suggesting that either a single pleiotropic locus or a  
379 cluster of loci in this region may be controlling both traits.

380

## 381 **Candidate genes and adaptive alleles within QTL regions**

### 382 *Cranial height*

383 Cranial height was the only trait with statistically significant or marginally significant QTL in  
384 both lakes (Figure 4,  $P < 0.1$ ). While the QTL occurred on different linkage groups between  
385 maps, we found a high degree of synteny between these linkage groups indicating that the QTL  
386 is located in the same genomic region in both lakes (**Table 2, Figure 3**). We also found the  
387 same overdominant genetic pattern in both lake crosses: heterozygotes showed increased cranial  
388 height relative to homozygous individuals (**Figure 5**).

389 We found 44 genes within scaffold 33 that fell partially or fully within the 95% credible  
390 intervals of the QTL in both lakes (Table 1, Table S1). Only three of these genes contained  
391 adaptive alleles within 20 kb: *wdr31*, *bri3bp*, and *gnaq* (**Table 3**). Interestingly, *gnaq* is well  
392 known to be associated with craniofacial development (Hall et al. 2007; Shirley et al. 2013) and  
393 is differentially expressed between our specialist species in developing larvae (McGirr and  
394 Martin 2020).

395

### 396 *Dentigerous Arm Width*

397 We found that regions on scaffolds 58 and 24 were associated with a significant QTL for  
398 dentigerous arm width in Little Lake and contained the max LOD scores for maxillary head  
399 protrusion and female mate preference in Crescent Pond (**Table 1, Table 2**). We found 161  
400 genes which fell partially or completely within these shared regions, but only 2 genes, *dysf* and  
401 *cyp26b1*, which contained adaptive alleles within 20 kbp (**Table 3**). The *dysf* gene provides  
402 instructions for making a protein called dysferlin, which is found in the sarcolemma membrane

403 that surrounds muscle fibers (Liu et al. 1998). This could indicate a role for muscle development  
404 in affecting skeletal development of the maxilla and premaxilla.

405

#### 406 *Dentigerous Arm Depth*

407 The QTL for dentigerous arm depth in Little Lake was associated with LG 6, which corresponds  
408 to LG 7 in Crescent Pond, however, no traits from Crescent Pond mapped to this linkage group  
409 (**Table 2, Figure 3**). Instead, dentigerous arm depth in Crescent Pond was associated with LG 13  
410 and did not share any similar genomic regions with those associated with dentigerous arm depth  
411 in Little Lake. We found 80 genes completely or partially within the 95% credible region for this  
412 QTL in Little Lak, but none contained adaptive alleles based on our criteria (Figure S1). In fact,  
413 only a single adaptive allele was found in this QTL region, but it was in an unannotated region of  
414 the genome (**Table 3**).

415

#### 416 *Maxillary Head Protrusion*

417 Maxillary head protrusion in Little Lake mapped to a QTL region on LG10 which corresponds to  
418 the max LOD scores for both lower jaw length and caudal peduncle height in Crescent Pond  
419 (**Table 2, Figure 3**). Across lakes, all three traits were associated with scaffolds 53, 2336, and  
420 6275. We found 528 genes partially or fully within these shared regions, but only 21 of these  
421 genes contained adaptive alleles within 20 kbp (**Table 3**). One of these genes, *twist1*, contains a  
422 non-synonymous substitution fixed in scale-eating pupfish on San Salvador Island, Bahamas  
423 (Richards et al. 2021). *Twist1* is a transcription factor and oncogene associated with palate  
424 development and oral jaw size in model organisms (Parsons et al. 2014; Teng et al. 2018).

425

426 *Jaw Closing In-Lever*

427 The QTL for jaw closing in-lever was associated with LG 9 in Little Lake, which corresponds to  
428 the max LOD scores for orbit diameter and anterior body depth in Crescent Pond (**Table 2**,  
429 **Figure 3**). Scaffolds 8 and 8020 were associated with all three of these traits. We found 13 genes  
430 which partially or completely fell within these shared regions, and only two genes, *map2k6* and  
431 *galr2*, which contained adaptive alleles within 20 kbp (**Table 3**). *Galr2* was also previously  
432 detected within a significant QTL for lower jaw length in pupfish (Martin et al. 2017).

433

434 *Dentigerous Arm Depth and Adductor Mandibulae Muscle Mass*

435 Finally, in Crescent Pond the QTL for dentigerous arm depth and adductor mandibulae muscle  
436 mass mapped to the exact same location on LG 13 (95% CI dentigerous arm depth (0, 250),  
437 adductor mandibulae muscle mass (0,70). This linkage group corresponds to LG14 in Little  
438 Lake, which contains the max LOD scores for both palatine height and suspensorium length  
439 (**Table 3**). We found 52 genes that overlapped between these regions, 18 of which contained  
440 adaptive alleles. Furthermore, three of the genes— *ube2w*, *ncoa2*, and *prlh*—contained adaptive  
441 alleles that introgressed from Laguna Bavaro in the Dominican Republic to snail-eating pupfish  
442 (*ube2w*), from Lake Cunningham, New Providence Island to scale-eating pupfish (*ncoa2*), or  
443 from North Carolina, USA to scale-eating pupfish (*prlh*). We also found four genes that  
444 contained adaptive alleles within 20 kbp that arose from de novo mutations: *cd226*, *cmb1*, *slc51a*,  
445 and *zfhx*; however, only one adaptive allele in *slc51a* is found within a coding region.

446

447 **Origins of adaptive alleles**

448 Adaptive alleles originating from standing genetic variation across the Caribbean were most  
449 common within shared QTL regions between lakes (86.03% within scale-eater populations, and  
450 53.32% within snail-eating populations; **Table 3**). However, observed proportions within shared  
451 QTL were significantly less than expected by chance (scale-eater expected 95% CI: (88.33%-  
452 90.37%), snail-eater expected 95% CI: (62%-67%;10,000 bootstrapped iterations). Instead, we  
453 found more introgressed scale-eater and snail-eater adaptive variants in shared QTL regions than  
454 expected by chance (Scale-eater observed: 12.13% introgressed, scale-eater expected 95% CI:  
455 (7.96%-9.88%); Snail-eater observed: 46.67% introgressed, snail-eater expected 95% CI:  
456 (32.22%-37.06%)). Finally, we found that about 1.83% of adaptive alleles within overlapping  
457 regions between lakes originated from de novo mutations in scale-eaters, however, this fell  
458 within the predicted null range (95% CI: (1.29%-2.17%)).

459

## 460 **Discussion**

### 461 **Parallel genetic changes underlie 5 out of 6 of craniofacial QTL**

462 We found evidence supporting both parallel and non-parallel genetic changes in an adaptive  
463 radiation of trophic specialist pupfishes. A single significant QTL was associated with cranial  
464 height in both lakes and mapped to the same genomic region, suggesting that parallel genetic  
465 changes are responsible for variation in this trait in both lakes. On the other hand, significant  
466 QTLs were identified for premaxilla dentigerous arm depth in each lake, but they mapped to  
467 different locations, indicating that this trait is associated with non-parallel genetic changes. We  
468 found an additional three traits with significant QTLs (dentigerous arm width, jaw closing in-  
469 lever, maxillary head protrusion) in the Little Lake population that were not detected in Crescent  
470 Pond. However, all genomic regions associated with these traits in Little Lake also mapped to

471 the max LOD score for this same integrated suite of craniofacial traits in Crescent Pond.  
472 Therefore, rather than assume independent QTL for each trait, we conservatively conclude that  
473 the same genomic regions are being reused in each lake and affect a highly integrated suite of  
474 craniofacial traits. Overall, we found that 5 out of the 6 significant QTLs were reused in some  
475 way across lakes suggesting that parallel genetic changes underly adaptive phenotypes in the San  
476 Salvador Island pupfish radiation.

477

#### 478 **High level of QTL reuse across ponds**

479 Overall, we found that about 16% (1 out of 6) of the identified QTL regions corresponded to  
480 non-parallel changes and 84% (5 out of 6) corresponded to parallel genetic changes—either  
481 affecting the same phenotypic trait or a tightly correlated craniofacial trait— across populations.  
482 The presence of both non-parallel and parallel genetic changes leading to convergent phenotypes  
483 across lakes has been documented previously. For example, Colosimo et al. (2004) investigated  
484 the genetic basis of armor plate morphology in two independent threespine stickleback  
485 populations and found a single large effect locus on LG 4 in the two populations. However, they  
486 also noted a potential difference in the dominance relationships of alleles across ponds at this  
487 location, and found additional differences in modifier QTLs between populations, suggesting  
488 that both parallel and non-parallel genetic changes could lead to the loss of armor plating.  
489 Similarly, Erickson et al. (2016) found evidence for both parallel (43% of QTL regions  
490 overlapped between at least two populations) and non-parallel (57% of QTL regions were found  
491 in only a single population) evolution in a QTL study investigating the genetic basis of 36  
492 skeletal phenotypes in three independent threespine stickleback populations. However, our  
493 findings suggest that pupfish exhibit a much higher proportion of parallel evolution than

494 previously documented in stickleback. In fact, Conte et al. (2012) estimated that the probability  
495 of convergence via gene reuse is only 32-55% —which is 1.5 to 2.5 times lower than our current  
496 finding— although this may be underestimated (Stern 2013).

497 Pufffish may have a higher rate of parallel evolution than other model fish speciation  
498 systems for a few reasons. First, the pufffish radiation is recent, although comparable in age to  
499 glacial stickleback populations, with specialist species diverging less than 10kya (Hagey and  
500 Mylroie 1995; Martin and Wainwright 2013), and parallel evolution is predicted to be more  
501 likely when populations or species have recently diverged (Rosenblum et al. 2014). This may be  
502 because recently diverged species are more likely to experience similar environments, have  
503 access to similar pools of genetic variation (either due to standing genetic variation or  
504 introgression), or similar genetic constraints. Second, the genomic basis of pufffish skeletal traits  
505 may be primarily controlled by cis-regulatory elements, which evolve more quickly and have  
506 less negative pleiotropy which may make them more likely to undergo parallel evolution (Stern  
507 and Orgogozo 2008). However, a previous study of allele-specific expression in the pufffish  
508 system found strong evidence that two cis-regulatory alleles were associated with skeletal  
509 development, but trans-acting elements predominated overall (McGirr and Martin 2021).

510 In part, the increased proportion of parallel evolution estimated in this study results from  
511 our relaxed thresholds for detecting and categorizing shared QTL regions. Previous QTL studies  
512 have typically searched for evidence of parallel evolution by only looking for one-to-one  
513 mapping in which the same genomic regions are associated with the same trait across  
514 populations at a genome-wide level of significance in each (Colosimo et al. 2004; Conte et al.  
515 2012). While this method provides the most clear-cut examples of parallel evolution, we argue  
516 that it vastly underestimates its frequency in nature. For example, this method would not

517 consider reuse of the same genomic regions for integrated morphological traits as parallel  
518 evolution, a pattern seen in this study and in Erickson et al. (2016). Furthermore, the strict one-  
519 to-one significance method for detecting parallel evolution does not include consideration of the  
520 hierarchy and diversity of convergence and parallel evolution, which can span morphological  
521 traits, ecotypes, performance, or even fitness (James et al. 2020; Rosenblum et al., 2014; Stern,  
522 2013; Martin and Wainwright 2013). Ultimately, we argue that our method of quantifying  
523 parallel evolution provides a more wholistic view of the process and better captures the  
524 frequency of reuse of adaptive genetic variation in nature.

525

### 526 **Few QTL may affect many highly integrated craniofacial traits**

527 There are several processes that may cause the same genomic regions to be associated with  
528 different traits between lakes. First, these genomic regions may be highly pleiotropic and affect  
529 several traits simultaneously. For example, Albert et al. (2007) found that that on average a  
530 single QTL affected 3.5 phenotypic traits in an analysis of 54 body traits in three-spine  
531 stickleback. Wagner et al. (2008) found a similar pattern in QTL analyses of 70 skeletal traits in  
532 mice, where a single QTL affected on average 7.8 phenotypic traits (the maximum being 30).

533 A second possibility is that a single QTL region may contain several tightly linked  
534 causative variants that are responsible for variation in many traits. Correlated phenotypic traits  
535 are generally assumed to have a shared genetic basis, but it is extremely difficult to determine if  
536 this is due to pleiotropy or tight linkage between genomic regions (Lynch and Walsh 1998;  
537 Gardner and Latta 2007; Paaby and Rockman 2013; Wright et al. 2010).

538 Finally, it may be that differences in methodology or sample sizes between lakes enable  
539 us to detect significant QTL for some traits in one lake and not the other. For example, our

540 analyses of Little Lake allowed us to detect significant QTL for effect sizes greater than 6.54  
541 PVE at 80% power, but we could only detect significant QTL for effect sizes greater than 8.41  
542 PVE at 80% power in Crescent Pond due to our lower sample size for this cross (Sen et al.  
543 2007). However, this level of power is typical in many non-model QTL studies (Ashton et al.  
544 2017). The ability to detect a significant QTL in one lake but not the other may be further  
545 explained by our use of different sequencing methods between populations. However, a critical  
546 component of our analyses involved searching for regions within 10 kbp of one another across  
547 maps to provide confidence that if we detected a significant QTL in one lake and not the other  
548 that it was not simply because that genomic region was not captured by the sequencing. For  
549 example, in Little Lake we detected a significant QTL associated with dentigerous arm depth on  
550 LG 6 but did not find any traits associated with this region of the genome in Crescent Pond.

551

### 552 **QTL are associated with different craniofacial traits across different lakes**

553 In this study we found an intriguing pattern of different traits mapping to the same region of the  
554 genome across lake populations. One potential explanation for this is that there are different  
555 relationships between traits in each lake, and we find some evidence of this in our phenotypic  
556 data. Figure S2 depicts correlation matrices between traits in 1) Little Lake and 2) Crescent  
557 Pond, and  $\chi^2$  comparisons of these two matrices reveals that the relationship between traits  
558 varies significantly between lakes ( $\chi^2=3135.99$ ,  $df = 756$ ,  $P < 3.6e-29$ ). For example, the  
559 relationship between maxillary head protrusion and lower jaw length is more than two times  
560 stronger in Little Lake compared to Crescent Pond (Pearson's  $r_{LL}=0.27$ , Pearson's  $r_{CP} = 0.12$ ),  
561 the relationship between dentigerous arm depth and suspensorium length is 1.8 times stronger in  
562 Little Lake than in Crescent Pond (Pearson's  $r_{LL}=0.45$ , Pearson's  $r_{CP} = 0.24$ ), and the relationship

563 between jaw closing in-lever and anterior body depth is more than two times stronger in Crescent  
564 Pond than in Little Lake (Pearson's  $r_{CP} = 0.23$ , Pearson's  $r_{LL}=0.11$ ).

565 This pattern may be explained by different epistatic interactions in each lake. For  
566 example, Juenger et al. (2005) detected significant QTL-QTL interactions in one mapping  
567 population of *Arabidopsis* but found no evidence of the same interactions in the other population.  
568 When we investigated the relationship between phenotype and genotype for cranial height, we  
569 found the same overdominance pattern in both lakes (Figure 5). However, the presence of  
570 epistatic interactions may also be an obstacle for QTL detection. In a mapping study of body  
571 weight in chicken, Carlborg et al. (2006) were only able to detect a single weak QTL despite the  
572 extremely divergent phenotypes between parental lines. However, when accounting for epistatic  
573 interactions, Carlborg et al. identified several additional significant QTL regions that explained a  
574 large amount of variation in body weights.

575 Finally, our method for searching for putative QTL regions may have led to this pattern.  
576 Similar studies have searched for influential genomic regions by first identifying a putative QTL  
577 in a single population, and then searching the already identified linkage group in the second  
578 population for any signal of a QTL associated with the same phenotype, often using relaxed  
579 LOD thresholds closer to the suggestive cut-off (LOD > 1.8, e.g., Erickson et al. 2016). Our  
580 approach, however, independently identified the positions of maximum LOD for all traits across  
581 the entire linkage map before searching for similar implicated regions between populations. We  
582 argue that our approach minimizes bias, because there are no prior expectations about which  
583 traits should be associated with a given genomic region within a suite of integrated traits, and  
584 reduces false positives because we only examine the maximum LOD position for each trait.  
585

## 586 **Identifying causative regions within QTL**

587 Multiple mapping populations across lakes may also be particularly useful for identifying  
588 candidate causal alleles. We found that one out of our six unique QTL regions mapped to the  
589 same genomic location across lakes and was associated with the same phenotypic trait—cranial  
590 height (Figure 4). In Crescent Pond, we found that a region of 110 cM was associated with this  
591 trait (LG10, position: 204, 95% CI (130,340)), which contained 426 genes. However, when we  
592 compared this region to the region independently identified in our Little Lake analysis, we found  
593 that the overlapping region was reduced to 20cM (LG1, position: 259, 95% CI (250-270)) and  
594 contained only 44 genes—a reduction of more than 80%. We found a similar pattern in the  
595 additional four QTL regions that mapped to the same genomic location across maps but were  
596 associated with different phenotypic traits and observed an average 56% reduction in region size.  
597 As noted above, Erickson et al. (2016) used a similar method of identifying candidate QTL  
598 regions across three hybrid populations of stickleback, and found that 43% of identified QTL  
599 regions were shared across two or more populations; however, they did not investigate whether  
600 these QTL regions completely or partially overlapped.

601 We also searched for adaptive alleles within QTL region that were identified in a  
602 previous study as 1) nearly fixed between species ( $F_{st} > 0.95$ ) and 2) showed significant evidence  
603 of a hard selective sweep (Richards et al. 2021). Overall, we found 789 shared genes within  
604 shared QTL regions across lakes, and that 45 of those genes contained adaptive variants (5.7%).  
605 This is a six-fold increase from the genome-wide expectation of 0.91% (176 genes associated  
606 with at least one adaptive variant / 19304 annotated genic regions), suggesting that these specific  
607 regions are important for adaptation to scale- and snail-feeding in wild pupfish. For example, a  
608 variant in *twist1* was found within the region associated with maxillary head protrusion in Little

609 Lake (which also overlapped with lower jaw length and caudal peduncle height in Crescent  
610 Pond). In model organisms, *twist1* is associated with palate and jaw development (Parsons et al.  
611 2014; Teng et al. 2018), and previous genome-wide association scans in pupfish showed that a  
612 region containing *twist1* was significantly associated with oral jaw size in the system (Richards  
613 et al. 2021). Similarly, we found that variants associated with *galr2* fell within the QTL region  
614 associated with jaw closing in-lever in Little Lake (which also overlapped with regions  
615 associated with orbit diameter and anterior body depth in Crescent Pond; scaffolds 8 and 8020),  
616 and previous QTL mapping studies, gene expression studies, and genome-wide association  
617 analyses have all implicated regions containing *galr2* with oral jaw development in pupfish  
618 (McGirr and Martin 2016; Martin et al. 2017; Richards et al. 2021).

619

### 620 **Increased use of introgressed adaptive variants in QTL regions**

621 We found that most genetic variation within shared QTL regions was also segregating across  
622 outgroup Caribbean generalist populations characterized by Richards et al. (2021; 86.04% within  
623 scale-eater populations, and 53.32% within snail-eating populations). Furthermore, we found  
624 more introgressed adaptive alleles from both scale-eater (observed: 12.13% introgressed,  
625 expected 95% CI: (7.96%-9.88%)) and snail-eater populations in shared QTL regions than  
626 expected by chance (observed: 46.67%, expected 95% CI: (32.22%-37.06%)). This supports the  
627 prediction that standing genetic variation and introgressed variation should underlie parallel  
628 genetic changes (Stern 2013; Thompson et al. 2019). Finally, we found that only 1.83% of  
629 adaptive alleles within shared QTL regions across both lakes originated from de novo mutations  
630 on San Salvador Island. While this percentage did not differ significantly from the expected

631 estimates (expected 95% CI: 1.3%-2.17%) it does not eliminate the possibility that de novo  
632 mutations play an important adaptive role in pupfish evolution.

633

### 634 **Conclusion**

635 In conclusion, we found that a single QTL region was responsible for variation in cranial height  
636 in both populations, and an additional four QTL regions were responsible for variation in  
637 different craniofacial traits across lakes, suggesting that parallel genetic changes underlie  
638 integrated suites of adaptive craniofacial phenotypes on San Salvador Island. Adaptive alleles  
639 were more commonly found within these detected QTL regions, and more of these adaptive  
640 alleles arrived on SSI via introgression than expected by chance. Finally, we argue that  
641 investigating QTL regions across populations in concert with estimation of hard selective sweeps  
642 in wild populations is a powerful tool for identifying potential causative regions of the genome  
643 affecting adaptive divergence.

644

### 645 **Acknowledgements**

646 We thank the University of California, Davis, the University of California, Berkeley, the  
647 University of North Carolina at Chapel Hill, NSF CAREER 1749764, NIH 5R01DE027052-02,  
648 and BSF 2016136 for funding to CHM. The Bahamas Environmental Science and Technology  
649 Commission and the Ministry of Agriculture provided permission to export fish and conduct this  
650 research. Rochelle Hanna, Velda Knowles, Troy Day, and the Gerace Research Centre provided  
651 logistical assistance in the field. All animal care protocols were approved by the University of  
652 California, Davis and the University of California, Berkeley Animal Care

653

654 **Author Contributions**

655 MESJ and CHM designed research; MESJ, CHM, JCD, and SR performed data collection; MESJ  
656 and EJR performed data analysis; MESJ and CHM wrote the paper. CHM provided funding.

657

658 **Data Accessibility**

659 Data will be deposited to Dryad and NCBI. Genomes are archived at the National Center for  
660 Biotechnology Information BioProject Database (Accessions:

661 PRJNA690558; PRJNA394148, PRJNA391309; and PRJNA305422).

662

663

664

**References**

- Alachiotis, N., A. Stamatakis, and P. Pavlidis. 2012. OmegaPlus: A scalable tool for rapid detection of selective sweeps in whole-genome datasets. *Bioinformatics* 28:2274–2275. Oxford Academic.
- Albert, A. Y. K., S. Sawaya, T. H. Vines, A. K. Knecht, C. T. Miller, B. R. Summers, S. Balabhadra, D. M. Kingsley, and D. Schluter. 2007. The genetics of adaptive shape shift in stickleback: pleiotropy and effect size. *Evolution* (N. Y). 0:071115145922005-??? John Wiley & Sons, Ltd.
- Ashton, D. T., P. A. Ritchie, and M. Wellenreuther. 2017. Fifteen years of quantitative trait loci studies in fish: challenges and future directions. *Mol. Ecol.* 26:1465–1476.
- Beavis, W. D. 1998. QTL analyses: power, precision, and accuracy. Pp. 145–162 *in* *Molecular dissection of complex traits*.
- Besnard, G., A. M. Muasya, F. Russier, E. H. Roalson, N. Salamin, and P. A. Christin. 2009. Phylogenomics of C4 photosynthesis in sedges (Cyperaceae): Multiple appearances and genetic convergence. *Mol. Biol. Evol.* 26:1909–1919. Oxford Academic.
- Bolnick, D. I., R. D. H. Barrett, K. B. Oke, D. J. Rennison, and Y. E. Stuart. 2018. (Non)Parallel evolution. *Annual Reviews Inc.*
- Bricelj, V. M., L. Connell, K. Konoki, S. P. MacQuarrie, T. Scheuer, W. A. Catterall, and V. L. Trainer. 2005. Sodium channel mutation leading to saxitoxin resistance in clams increases risk of PSP. *Nature* 434:763–767. Nature Publishing Group.
- Broman, K. W., D. M. Gatti, P. Simecek, N. A. Furlotte, P. Prins, S. Sen, B. S. Yandell, and G. A. Churchill. 2019. R/qt2: Software for mapping quantitative trait loci with high-dimensional data and multiparent populations. *Genetics* 211:495–502. Genetics Society of America.

- Broman, K. W., H. Wu, S. Sen, and G. A. Churchill. 2003. R/qtl: QTL mapping in experimental crosses. *Bioinformatics* 19:889–890. Oxford Academic.
- Buckland, S. T., A. C. Davison, and D. V. Hinkley. 1998. Bootstrap Methods and Their Application. *Biometrics* 54:795.
- Canty, A., and B. D. Ripley. 2021. boot: Bootstrap R (S-Plus) Functions. R Packag. version 1.3-28.
- Carlborg, Ö., L. Jacobsson, P. Åhgren, P. Siegel, and L. Andersson. 2006. Epistasis and the release of genetic variation during long-term selection. *Nat. Genet.* 38:418–420. Nature Publishing Group.
- Chan, Y. F., M. E. Marks, F. C. Jones, G. Villarreal, M. D. Shapiro, S. D. Brady, A. M. Southwick, D. M. Absher, J. Grimwood, J. Schmutz, R. M. Myers, D. Petrov, B. Jónsson, D. Schluter, M. A. Bell, and D. M. Kingsley. 2010. Adaptive evolution of pelvic reduction in sticklebacks by recurrent deletion of a pitxl enhancer. *Science* (80-. ). 327:302–305. American Association for the Advancement of Science.
- Chen, L., A. L. Devries, and C. H. C. Cheng. 1997. Convergent evolution of antifreeze glycoproteins in Antarctic notothenioid fish and Arctic cod. *Proc. Natl. Acad. Sci. U. S. A.* 94:3817–3822.
- Christin, P. A., N. Salamin, V. Savolainen, M. R. Duvall, and G. Besnard. 2007. C4 Photosynthesis Evolved in Grasses via Parallel Adaptive Genetic Changes. *Curr. Biol.* 17:1241–1247. Cell Press.
- Colosimo, P. F., C. L. Peichel, K. Nereng, B. K. Blackman, M. D. Shapiro, D. Schluter, and D. M. Kingsley. 2004. The genetic architecture of parallel armor plate reduction in threespine sticklebacks. *PLoS Biol.* 2:e109. Public Library of Science.
- Conte, G. L., M. E. Arnegard, C. L. Peichel, and D. Schluter. 2012. The probability of genetic parallelism and convergence in natural populations. *Proc. R. Soc. B Biol. Sci.* 279:5039–5047. Royal Society.
- Cresko, W. A., A. Amores, C. Wilson, J. Murphy, M. Currey, P. Phillips, M. A. Bell, C. B. Kimmel, and J. H. Postlethwait. 2004. Parallel genetic basis for repeated evolution of armor loss in Alaskan threespine stickleback populations. *Proc. Natl. Acad. Sci. U. S. A.* 101:6050–6055.
- Depristo, M. A., E. Banks, R. Poplin, K. V Garimella, J. R. Maguire, C. Hartl, A. A. Philippakis, G. Del Angel, M. A. Rivas, M. Hanna, A. McKenna, T. J. Fennell, A. M. Kernysky, A. Y. Sivachenko, K. Cibulskis, S. B. Gabriel, D. Altshuler, and M. J. Daly. 2011. A framework for variation discovery and genotyping using next-generation DNA sequencing data. *Nat. Genet.* 43:491–501.
- Dingerkus, G., and L. D. Uhler. 1977. Stain Technology Enzyme Clearing of Alcian Blue Stained Whole Small Vertebrates for Demonstration of Cartilage. , doi: 10.3109/10520297709116780.
- Donley, J. M., C. A. Sepulveda, P. Konstantinidis, S. Gemballa, and R. E. Shadwick. 2004. Convergent evolution in mechanical design of lamnid sharks and tunas. *Nature* 429:61–65.
- Echelle, A. A., and A. E. Echelle. 2020. Cyprinodontidae: Pupfishes. Pp. 609–673 in *Freshwater Fishes of North America*. The Johns Hopkins University Press.
- Erickson, P. A., A. M. Glazer, E. E. Killingbeck, R. M. Agoglia, J. Baek, S. M. Carsanaro, A. M. Lee, P. A. Cleves, D. Schluter, and C. T. Miller. 2016. Partially repeatable genetic basis of benthic adaptation in threespine sticklebacks. *Evolution* (N. Y). 70:887–902.
- Feldman, C. R., E. D. Brodie, E. D. Brodie, and M. E. Pfrender. 2012. Constraint shapes

- convergence in tetrodotoxinresistant sodium channels of snakes. *Proc. Natl. Acad. Sci. U. S. A.* 109:4556–4561.
- Feldman, C. R., E. D. Brodie, E. D. Brodie, and M. E. Pfrender. 2009. The evolutionary origins of beneficial alleles during the repeated adaptation of garter snakes to deadly prey. *Proc. Natl. Acad. Sci. U. S. A.* 106:13415–13420.
- Feulner, P. G. D., F. J. J. Chain, M. Panchal, C. Eizaguirre, M. Kalbe, T. L. Lenz, M. Mundry, I. E. Samonte, M. Stoll, M. Milinski, T. B. H. Reusch, and E. Bornberg-Bauer. 2013. Genome-wide patterns of standing genetic variation in a marine population of three-spined sticklebacks. *Mol. Ecol.* 22:635–649.
- Futuyma, D. J. 1986. *Evolutionary Biology*. 2d ed. Sinauer, Sunderland, Mass.
- Gardner, K. M., and R. G. Latta. 2007. Shared quantitative trait loci underlying the genetic correlation between continuous traits. *Mol. Ecol.* 16:4195–4209. John Wiley & Sons, Ltd.
- Grant, P. R., B. R. Grant, J. A. Markert, L. F. Keller, and K. Petren. 2004. Convergent evolution of Darwin’s finches caused by introgressive hybridization and selection. *Evolution (N. Y.)* 58:1588–1599. Society for the Study of Evolution.
- Haenel, Q., M. Roesti, D. Moser, A. D. C. MacColl, and D. Berner. 2019. Predictable genome-wide sorting of standing genetic variation during parallel adaptation to basic versus acidic environments in stickleback fish. *Evol. Lett.* 3:28–42. Wiley.
- Hagey, F. M., and J. E. Myroie. 1995. Pleistocene lake and lagoon deposits, San Salvador island, Bahamas. *Spec. Pap. Soc. Am.* 77–90.
- Haley, C. S., and S. A. Knott. 1992. A simple regression method for mapping quantitative trait loci in line crosses using flanking markers. *Heredity (Edinb.)* 69:315–324.
- Hall, B. D., R. G. Cadle, S. M. Morrill-Cornelius, and C. A. Bay. 2007. Phacomatosis pigmentovascularis: Implications for severity with special reference to Mongolian spots associated with Sturge-Weber and Klippel-Trenaunay syndromes. Pp. 3047–3053 in *American Journal of Medical Genetics, Part A*. John Wiley & Sons, Ltd.
- Hedrick, P. W. 2013. Adaptive introgression in animals: Examples and comparison to new mutation and standing variation as sources of adaptive variation. John Wiley & Sons, Ltd.
- Hedrick, T. L. 2008. Software techniques for two- and three-dimensional kinematic measurements of biological and biomimetic systems. *Bioinspiration and Biomimetics* 3.
- Hernandez, L. P., D. Adriaens, C. H. Martin, P. C. Wainwright, B. Masschaele, and M. Dierick. 2018. Building trophic specializations that result in substantial niche partitioning within a young adaptive radiation. *J. Anat.* 232:173–185.
- Hopkins, C. D. 1995. Convergent designs for electrogenesis and electroreception. *Curr. Opin. Neurobiol.* 5:769–777.
- James, M. E., M. J. Wilkinson, H. L. North, J. Engelstädter, and D. Ortiz-Barrientos. 2020. A framework to quantify phenotypic and genotypic parallel evolution. *bioRxiv*, doi: 10.1101/2020.02.05.936450.
- Jones, F. C., M. G. Grabherr, Y. F. Chan, P. Russell, E. Mauceli, J. Johnson, R. Swofford, M. Pirun, M. C. Zody, S. White, E. Birney, S. Searle, J. Schmutz, J. Grimwood, M. C. Dickson, R. M. Myers, C. T. Miller, B. R. Summers, A. K. Knecht, S. D. Brady, H. Zhang, A. A. Pollen, T. Howes, C. Amemiya, J. Baldwin, T. Bloom, D. B. Jaffe, R. Nicol, J. Wilkinson, E. S. Lander, F. Di Palma, K. Lindblad-Toh, and D. M. Kingsley. 2012. The genomic basis of adaptive evolution in threespine sticklebacks. *Nature* 484:55–61.
- Jost, M. C., D. M. Hillis, Y. Lu, J. W. Kyle, H. A. Fozzard, and H. H. Zakon. 2008. Toxin-resistant sodium channels: Parallel adaptive evolution across a complete gene family. *Mol.*

- Biol. Evol. 25:1016–1024. Oxford Academic.
- Juenger, T. E., S. Sen, K. A. Stowe, and E. L. Simms. 2005. Epistasis and genotype-environment interaction for quantitative trait loci affecting flowering time in *Arabidopsis thaliana*. Pp. 87–105 in *Genetica*.
- Katz, P. S. 2006. *Comparative Neurophysiology: An Electric Convergence in Fish*.
- Kowalko, J. E., N. Rohner, T. A. Linden, S. B. Rompani, W. C. Warren, R. Borowsky, C. J. Tabin, W. R. Jeffery, and M. Yoshizawa. 2013. Convergence in feeding posture occurs through different genetic loci in independently evolved cave populations of *Astyanax mexicanus*. *Proc. Natl. Acad. Sci. U. S. A.* 110:16933–16938.
- Lander, E., and L. Kruglyak. 1995. Genetic dissection of complex traits: Guidelines for interpreting and reporting linkage results. *Nat. Genet.* 11:241–247.
- Lander, E. S., and S. Botstein. 1989. Mapping mendelian factors underlying quantitative traits using RFLP linkage maps. *Genetics* 121:185.
- Linnen, C. R., Y. P. Poh, B. K. Peterson, R. D. H. Barrett, J. G. Larson, J. D. Jensen, and H. E. Hoekstra. 2013. Adaptive evolution of multiple traits through multiple mutations at a single gene. *Science (80-. )*. 339:1312–1316. American Association for the Advancement of Science.
- Liu, J., M. Aoki, I. Illa, C. Wu, M. Fardeau, C. Angelini, C. Serrano, J. Andoni Urtizberea, F. Hentati, M. Ben Hamida, S. Bohlega, E. J. Culper, A. A. Amato, K. Bossie, J. Oeltjen, K. Bejaoui, D. McKenna-Yasek, B. A. Hosler, E. Schurr, K. Arahata, P. J. De Jong, and R. H. Brown. 1998. Dysferlin, a novel skeletal muscle gene, is mutated in Miyoshi myopathy and limb girdle muscular dystrophy. *Nat. Genet.* 20:31–36.
- Liu, R. K., and A. A. Echelle. 2013. Behavior of the Catarina pupfish (cyprinodontidae: *Megupsilon aporus*), a severely imperiled species. *Southwest. Nat.* 58:1–7. Southwestern Association of Naturalists.
- Losos, J. B. 2009. *Lizards in an Evolutionary Tree: Ecology and Adaptive Radiation of Anoles*. University of California Press, Berkeley.
- Lynch, M., and B. Walsh. 1998. *Genetics and Analysis of Quantitative Traits*. Vol. 1. Sinauer Associates, Sunderland, MA, Sunderland, MA.
- Marsden, C. D., Y. Lee, K. Kreppel, A. Weakley, A. Cornel, H. M. Ferguson, E. Eskin, and G. C. Lanzaro. 2014. Diversity, differentiation, and linkage disequilibrium: Prospects for association mapping in the malaria vector *Anopheles arabiensis*. *G3 Genes, Genomes, Genet.* 4:121–131. Genetics Society of America.
- Martin, C. H., J. E. Crawford, B. J. Turner, and L. H. Simons. 2016. Diabolical survival in Death Valley: recent pupfish colonization, gene flow and genetic assimilation in the smallest species range on earth. *Proc. R. Soc. B Biol. Sci.* 283:20152334.
- Martin, C. H., J. S. Cutler, J. P. Friel, C. Dening Touokong, G. Coop, and P. C. Wainwright. 2015. Complex histories of repeated gene flow in Cameroon crater lake cichlids cast doubt on one of the clearest examples of sympatric speciation. *Evolution (N. Y.)*. 69:1406–1422.
- Martin, C. H., P. A. Erickson, and C. T. Miller. 2017. The genetic architecture of novel trophic specialists: larger effect sizes are associated with exceptional oral jaw diversification in a pupfish adaptive radiation. *Mol. Ecol.* 26:624–638.
- Martin, C. H., and L. C. Feinstein. 2014. Novel trophic niches drive variable progress towards ecological speciation within an adaptive radiation of pupfishes. *Mol. Ecol.* 23:1846–1862.
- Martin, C. H., and P. C. Wainwright. 2013. A Remarkable Species Flock of *Cyprinodon* Pupfishes Endemic to San Salvador Island, Bahamas. *Bull. Peabody Museum Nat. Hist.*

54:231–241.

- McGirr, J. A., and C. H. Martin. 2020. Ecological divergence in sympatry causes gene misexpression in hybrids. *Mol. Ecol.* 29:2707–2721.
- McGirr, J. A., and C. H. Martin. 2021. Few Fixed Variants between Trophic Specialist Pupfish Species Reveal Candidate Cis-Regulatory Alleles Underlying Rapid Craniofacial Divergence. *Mol. Biol. Evol.* 38:405–423.
- McGirr, J. A., and C. H. Martin. 2016. Novel candidate genes underlying extreme trophic specialization in Caribbean pupfishes. *Mol. Biol. Evol.* 34:msw286. Narnia.
- Morjan, C. L., and L. H. Rieseberg. 2004. How species evolve collectively: implications of gene flow and selection for the spread of advantageous alleles. *Mol. Ecol.* 13:1341–1356. John Wiley & Sons, Ltd.
- Nelson, T. C., and W. A. Cresko. 2018. Ancient genomic variation underlies repeated ecological adaptation in young stickleback populations. *Evol. Lett.* 2:9–21.
- Nyholt, D. R. 2000. All LODs are not created equal. *Am. J. Hum. Genet.* 67:282–288. University of Chicago Press.
- O’brown, N. M., B. R. Summers, F. C. Jones, S. D. Brady, and D. M. Kingsley. 2015. A recurrent regulatory change underlying altered expression and Wnt response of the stickleback armor plates gene EDA. *Elife* 2015.
- Orr, H. A. 2006. The distribution of fitness effects among beneficial mutations in Fisher’s geometric model of adaptation. *J. Theor. Biol.* 238:279–285.
- Paaby, A. B., and M. V. Rockman. 2013. The many faces of pleiotropy. Elsevier Current Trends.
- Parsons, T. E., S. M. Weinberg, K. Khaksarfard, R. N. Howie, M. Elsalanty, J. C. Yu, and J. J. Cray. 2014. Craniofacial shape variation in Twist1<sup>+/-</sup> mutant mice. *Anat. Rec.* 297:826–833. Blackwell Publishing Inc.
- Pavlidis, P., D. Živković, A. Stamatakis, and N. Alachiotis. 2013. SweeD: Likelihood-based detection of selective sweeps in thousands of genomes. *Mol. Biol. Evol.* 30:2224–2234. *Mol Biol Evol.*
- Richards, E. J., and C. H. Martin. 2017. Adaptive introgression from distant Caribbean islands contributed to the diversification of a microendemic adaptive radiation of trophic specialist pupfishes. *PLoS Genet.* 13:e1006919.
- Richards, E. J., J. A. McGirr, J. R. Wang, M. E. St. John, J. W. Poelstra, M. J. Solano, D. C. O’Connell, B. J. Turner, and C. H. Martin. 2021. A vertebrate adaptive radiation is assembled from an ancient and disjunct spatiotemporal landscape. *Proc. Natl. Acad. Sci.* 118:e2011811118. Proceedings of the National Academy of Sciences.
- Risch, N. 1990. Linkage strategies for genetically complex traits. I. Multilocus models. *Am. J. Hum. Genet.* 46:222–228.
- Rosenblum, E. B., C. E. Parent, and E. E. Brandt. 2014. The molecular basis of phenotypic convergence. *Annu. Rev. Ecol. Evol. Syst.* 45:203–226.
- Russello, M. A., M. D. Waterhouse, P. D. Etter, and E. A. Johnson. 2015. From promise to practice: Pairing non-invasive sampling with genomics in conservation. *PeerJ* 2015:e1106. PeerJ Inc.
- Schluter, D., E. A. Clifford, M. Nemethy, and J. S. McKinnon. 2004. Parallel evolution and inheritance of quantitative traits. *Am. Nat.* 163:809–822. The University of Chicago Press.
- Sen, Ś., J. M. Satagopan, K. W. Broman, and G. A. Churchill. 2007. R/qtlDesign: Inbred line cross experimental design. *Mamm. Genome* 18:87–93.
- Shirley, M. D., H. Tang, C. J. Gallione, J. D. Baugher, L. P. Frelin, B. Cohen, P. E. North, D. A.

- Marchuk, A. M. Comi, and J. Pevsner. 2013. Sturge–Weber Syndrome and Port-Wine Stains Caused by Somatic Mutation in GNAQ . *N. Engl. J. Med.* 368:1971–1979. New England Journal of Medicine (NEJM/MMS).
- St. John, M. E., K. Dixon, and C. H. Martin. 2020a. Oral shelling within an adaptive radiation of pupfishes: testing the adaptive function of novel nasal protrusion and behavioral preference. *J. Fish Biol.* 1–9.
- St. John, M. E., R. Holzman, and C. H. Martin. 2020b. Rapid adaptive evolution of scale-eating kinematics to a novel ecological niche. *J. Exp. Biol.* jeb.217570.
- Stern, D. L. 2013. The genetic causes of convergent evolution. *Nat. Rev. Genet.* 14:751–764. Nature Publishing Group.
- Stern, D. L., and V. Orgogozo. 2008. The loci of evolution: How predictable is genetic evolution?
- Stevenson, M. M. 1981. Karyomorphology of Several Species of Cyprinodon. *Copeia* 1981:494. JSTOR.
- Stuart, Y. E., T. Veen, J. N. Weber, D. Hanson, M. Ravinet, B. K. Lohman, C. J. Thompson, T. Tasneem, A. Doggett, R. Izen, N. Ahmed, R. D. H. Barrett, A. P. Hendry, C. L. Peichel, and D. I. Bolnick. 2017. Contrasting effects of environment and genetics generate a continuum of parallel evolution. *Nat. Ecol. Evol.* 1:158. Nature Publishing Group.
- Taylor, J., and D. Butler. 2017. R package ASMap: Efficient genetic linkage map construction and diagnosis. *J. Stat. Softw.*, doi: 10.18637/jss.v079.i06.
- Taylor, R. S., M. Manseau, R. L. Horn, S. Keobouasone, G. B. Golding, and P. J. Wilson. 2020. The role of introgression and ecotypic parallelism in delineating intraspecific conservation units. *Mol. Ecol.* 29:2793–2809. Blackwell Publishing Ltd.
- Teng, C. S., M. C. Ting, D. T. Farmer, M. Brockop, R. E. Maxson, and J. G. Crump. 2018. Altered bone growth dynamics prefigure craniosynostosis in a zebrafish model of Saethre-Chotzen syndrome. *Elife* 7. eLife Sciences Publications Ltd.
- Thompson, K. A., M. M. Osmond, and D. Schluter. 2019. Parallel genetic evolution and speciation from standing variation. *Evol. Lett.* 3:129–141. Wiley.
- Wagner, G. P., J. P. Kenney-Hunt, M. Pavlicev, J. R. Peck, D. Waxman, and J. M. Cheverud. 2008. Pleiotropic scaling of gene effects and the “cost of complexity.” *Nature* 452:470–472. Nature Publishing Group.
- Wittkopp, P. J., B. L. Williams, J. E. Selegue, and S. B. Carroll. 2003. *Drosophila* pigmentation evolution: Divergent genotypes underlying convergent phenotypes. *Proc. Natl. Acad. Sci. U. S. A.* 100:1808–1813. National Academy of Sciences.
- Xie, K. T., G. Wang, A. C. Thompson, J. I. Wucherpfennig, T. E. Reimchen, A. D. C. MacColl, D. Schluter, M. A. Bell, K. M. Vasquez, and D. M. Kingsley. 2019. DNA fragility in the parallel evolution of pelvic reduction in stickleback fish. *Science* (80-. ). 363:81–84.
- Yang, J., N. A. Zaitlen, M. E. Goddard, P. M. Visscher, and A. L. Price. 2014. Advantages and pitfalls in the application of mixed-model association methods.
- Yu, J., G. Pressoir, W. H. Briggs, I. V. Bi, M. Yamasaki, J. F. Doebley, M. D. McMullen, B. S. Gaut, D. M. Nielsen, J. B. Holland, S. Kresovich, and E. S. Buckler. 2006. A unified mixed-model method for association mapping that accounts for multiple levels of relatedness. *Nat. Genet.* 38:203–208. Nature Publishing Group.

## Tables and Figures

**Table 1.** Maximum LOD scores for all 29 traits measured in Little Lake and Crescent Pond mapping crosses. A genome scan with a single-QTL model by Haley-Knott regression was used to identify the position with the highest LOD score, 95% Bayesian credible intervals, and the genome-wide significance level for each trait ( $P < 0.1$ : • ;  $P < 0.05$ : \*). We also report the scaffold numbers of genomic regions that fell within the 95% credible intervals associated with the maximum LOD position for each trait, the number of individuals phenotyped, percent variance explained (PVE) by the max LOD region, and the uncorrected  $P$ -value associated with each max LOD region.

Trait	Population	Scaffold	Max LOD	Genome - wide Significance	n	PVE	$\chi^2$ P-Value
Lower Jaw Length	Crescent Pond	53, 7087, 2336, 6275, 26, 7335	2.89		205	6.29	0.0013
	Little Lake	24, 4028, 58, 16	3.30		228	6.45	0.0005
	Crescent Pond	31, 4, 451, 19	3.60		204	7.81	0.0002
Jaw closing In-Lever	Little Lake	8, 9588, 8020	4.11	•	227	7.99	0.0001
	Crescent Pond	6086, 11	2.43		205	5.32	0.0037
Jaw Opening In-Lever	Little Lake	43	2.98		227	5.87	0.0010
	Crescent Pond	34, 22, 6304	2.90		205	6.31	0.0013
Palatine Height	Little Lake	11	2.73		228	5.36	0.0019
	Crescent Pond	46, 37, 31, 26, 60, 7556, 10198, 22	3.54		204	7.68	0.0003
Suspensorium Length	Little Lake	11	3.51		227	6.88	0.0003
	Crescent Pond	52, 13137, 40	2.19		202	4.87	0.0065
Dentigerous Arm Width	Little Lake	24, 4028, 58, 16	4.05	• *	228	7.85	0.0001
	Crescent Pond	27, 593, 4, 31, 451, 19	2.67		204	5.85	0.0021
Maxilla Length	Little Lake	56	3.03		228	5.94	0.0009
	Crescent Pond	27, 593, 4, 31, 451, 19	2.98		205	6.47	0.0011
Dentigerous Arm Base	Little Lake	26	3.70		228	7.21	0.0002

<b>Dentigerous Arm Depth</b>	Crescent Pond	6086, 11, 46	4.20	• *	205	9.00	0.0001
	Little Lake	5	3.70	•	217	7.55	0.0002
<b>Ascending Process Length</b>	Crescent Pond	27, 593, 4, 31, 451, 19	2.70		201	6.00	0.0020
	Little Lake	46, 37	3.70		210	7.79	0.0002
<b>Maxillary Head Height</b>	Crescent Pond	6086, 11, 46	2.33		205	5.11	0.0046
	Little Lake	7, 30	2.19		228	4.33	0.0064
<b>Ectopterygoid</b>	Crescent Pond	14, 9, 16, 5405, 11419	2.81		205	6.11	0.0016
	Little Lake	9	3.36		228	6.56	0.0004
<b>Maxillary Head Protrusion</b>	Crescent Pond	58, 24, 41, 47	2.70		205	5.88	0.0020
	Little Lake	7431, 53, 6275, 2336, 25	4.03	• *	228	7.82	0.0001
<b>Nasal Tissue Protrusion</b>	Crescent Pond	46, 37, 31, 26, 60, 7556, 10198, 22	2.25		205	4.93	0.0056
	Little Lake	9	3.69		228	7.18	0.0002
<b>Orbit Diameter</b>	Crescent Pond	9588, 8, 8020	2.34		205	5.13	0.0045
	Little Lake	52, 40, 41	2.58		227	5.10	0.0026
<b>Cranial Height</b>	Crescent Pond	33, 39	3.59	•	205	7.74	0.0003
	Little Lake	33	3.94	•	224	7.78	0.0001
<b>Head Depth</b>	Crescent Pond	16, 40	2.98		204	6.51	0.0010
	Little Lake	52, 40, 41	2.71		223	5.45	0.0019
<b>Pelvic Girdle Length</b>	Crescent Pond	31, 18, 15, 11057, 55, 52	2.68		203	5.90	0.0021
	Little Lake	27, 37, 7	2.87		226	5.68	0.0014
<b>Premaxilla Pelvic Girdle</b>	Crescent Pond	37, 46, 7556, 10198	3.15		202	6.92	0.0007
	Little Lake	35, 38, 20, 8508, 10278, 33	2.63		231	5.10	0.0024
<b>Standard</b>	Crescent	14, 9, 16, 5405,	2.90		204	6.34	0.0013

<b>Length (mm)</b>	Pond	11419				
	Little Lake	31, 46, 37	3.48	231	6.69	0.0003
<b>Cranium Dorsal Fin</b>	Crescent Pond	6704, 52, 13137, 40	2.84	205	6.18	0.0014
	Little Lake	37, 22, 7556	3.45	231	6.65	0.0004
<b>Dorsal Fin Width</b>	Crescent Pond	43, 26, 14743	2.18	205	4.78	0.0066
	Little Lake	842, 44, 1074, 6, 30	3.00	230	5.83	0.0010
<b>Dorsal Fin Height</b>	Crescent Pond	18, 31, 15, 11057, 55	2.84	203	6.23	0.0015
	Little Lake	43	3.50	222	7.00	0.0003
<b>Anterior Body Depth</b>	Crescent Pond	8, 8020	2.94	204	6.43	0.0011
	Little Lake	6094, 5, 4	3.33	230	6.45	0.0005
<b>Posterior Body Depth</b>	Crescent Pond	20, 471, 39, 8508, 33	2.86	203	6.27	0.0014
	Little Lake	18, 15	3.02	228	5.92	0.0009
<b>Caudal Peduncle Length</b>	Crescent Pond	31, 18, 15, 11057, 55, 52	2.87	203	6.30	0.0014
	Little Lake	24, 4028, 58, 16	2.16	230	4.23	0.0070
<b>Anal Fin Width</b>	Crescent Pond	18, 15, 11057, 55	2.89	201	6.41	0.0013
	Little Lake	6, 842, 44, 1074, 30	2.40	229	4.71	0.0040
<b>Anal Fin Height</b>	Crescent Pond	43, 26, 14743	2.93	201	6.48	0.0012
	Little Lake	8, 9588, 8020	3.15	229	6.14	0.0007
<b>Caudal Peduncle Height</b>	Crescent Pond	53, 7087, 2336, 6275, 26, 7335	1.97	205	4.32	0.0108
	Little Lake	47, 1962	3.32	230	6.44	0.0005
<b>Adductor</b>	Crescent Pond	6086, 11	3.56	170	9.18	0.0003
	Little Lake	-	-	-	-	-
<b>Proportion Time Spent Near Scale-Eater Mates</b>	Crescent Pond	58, 24, 41, 47	2.05	74	12.00	0.0089
	Little Lake	-	-	-	-	-

**Table 2.** Position of maximum LOD score and 95% credible intervals for each trait in the Little Lake linkage map and the Crescent Pond linkage map. Colors represent corresponding linkage groups across lakes. Asterisks represent traits that were marginally significant at the  $P < 0.1$  level in the genome scan.

Little Lake					Crescent Pond				
Trait	Sig.	LG	Position genomewide		Trait	Sig.	LG	Position genomewide	
			Max LOD score	95% CI				Max LOD score	95% CI
Cranial Height	*	1	259	(250,270)	Suspensorium Length	1	566	(20,730)	
Premaxilla to Pelvic Girdle		1	146	(0,350)	Nasal Tissue Protrusion	1	570	(0,740)	
Cranium to Dorsal Fin		2	303	(160,380)	Premaxilla to Pelvic Girdle	1	568	(310,600)	
Lower Jaw Length		3	9	(0,340)	Ectopterygoid	3	272	(0,560)	
Dentigerous Arm Width	*	3	9	(0,340)	Standard Length (mm)	3	50	(40,500)	
Caudal Peduncle Length		3	168	(0,340)	Dentigerous Arm Width	4	317	(40,510)	
Dorsal Fin width		4	187	(10,310)	Cranium to Dorsal Fin	4	89	(30,510)	
Anal Fin Width		4	14	(0,280)	Lower Jaw Length	5	136	(0,470)	
Dentigerous Arm Depth	*	6	79	(20,90)	Caudal Peduncle height	5	381	(0,470)	
Anterior Body Depth		6	289	(0,300)	Jaw Closing In-Lever	6	380	(150,410)	
Orbit Diameter		8	266	(0,290)	Maxilla Length	6	468	(0,480)	
Head Depth		8	206	(0,290)	Dentigerous Arm Base	6	107	(0,480)	
Jaw Closing In-Lever	*	9	54	(40,90)	Ascending Proces Length	6	106	(0,470)	
Anal Fin Height		9	100	(70,240)	Pelvic Girdle Length	8	370	(20,435)	
Maxillary Head Protrusion	*	10	35	(0,260)	Dorsal Fin Height	8	91	(0,380)	
Ascending Process Length		12	119	(90,150)	Caudal Peduncle Length	8	258	(30,425)	
Standard Length (mm)		12	200	(50,210)	Anal Fin Width	8	190	(110,400)	
Ectopterygoid		13	170	(150,180)	Maxillary Head Protrusion	9	300	(0,350)	
Nasal Tissue Protrusion		13	193	(20,200)	Proportion Time Spent Near Scale-Eater Males	9	166	(50,340)	
Palatine Height		14	147	(110,210)	Cranial Height	*	10	204	(130,340)
Suspensorium Length		14	153	(70,180)	Posterior Body Depth	10	270	(0,330)	
Jaw Opening In-Lever		16	58	(40,140)	Palatine Height	11	70	(0,310)	
Dorsal Fin Height		16	52	(40,60)	Head Depth	12	111	(100,280)	
Pelvic Girdle Length		17	50	(10,160)	Opening In-Lever	13	10	(0,90)	
Maxillary Head Height		18	122	(30,160)	Dentigerous Arm Depth	*	13	2	(0,250)
Caudal Peduncle Height		19	44	(20,90)	Maxillary Head Height	13	170	(0,280)	
Dentigerous Arm Base		21	74	(0,100)	Adductor Mandibulae Mass	*	13	2	(0,70)
Maxilla Length		22	40	(20,50)	Dorsal Fin Width	14	305	(30,330)	
Posterior Body Depth		24	30	(10,30)	Anal Fin Width	14	330	(280,330)	
					Orbit Diameter	16	107	(0,190)	
					Anterior Body Depth	16	170	(10,220)	

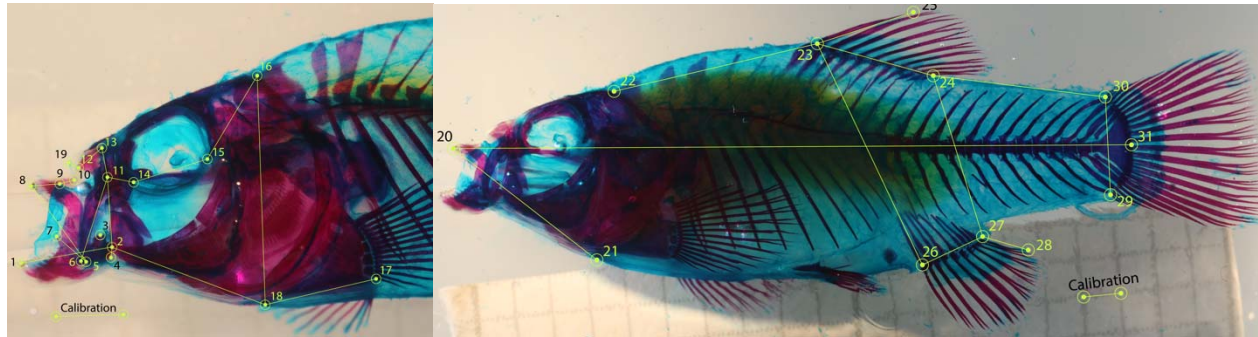
**Table 3.** Number of adaptive alleles and any genes within 20 kbp found in trait QTL with maximum LOD scores for both lakes. Adaptive alleles were categorized as either standing genetic variation (SGV), introgression (Intro.), or de novo mutations, and were estimated independently for snail-eaters and scale-eaters in a previous study (Richards et al. 2021). Asterisks represent traits that were significant at the  $P < 0.1$  level in the genome-wide scan, while crosses show traits that corresponded to the same locations in the alternate lake.

Traits	Gene	Snail-Eater		Scale-Eater		
		SGV	Intro.	SGV	Intro.	de novo
<b>Cranial Height*</b>	<i>bri3bp</i>	-	26	28	-	-
	<i>gnaq</i>	9	-	9	-	-
	<i>wdr31</i>	18	2	20	-	-
	Unannotated Regions	1	-	11	-	-
<b>Dentigerous Arm Width*</b>	<i>cyp26b1</i>	-	8	8	-	-
	<i>dysf</i>	-	-	1	-	-
<b>Female mate preferencet</b>	Unannotated Regions	-	67	216	-	1
<b>Maxillary Head Protrusion†</b>	Unannotated Regions	-	-	1	-	-
<b>Dentigerous Arm Depth*</b>	<i>cox6b1</i>	8	-	8	-	-
	<i>cyp21a2</i>	-	-	2	-	-
	<i>eva1b</i>	-	-	2	-	-
	<i>fhod3</i>	-	-	2	-	-
	<i>galnt1</i>	-	-	-	17	-
	<i>glipr2</i>	-	-	3	-	-
	<i>hdac9b</i>	-	-	-	1	-
	<i>mag</i>	-	-	2	-	-
	<i>map7d1</i>	25	-	25	-	-
	<i>mindy3</i>	-	-	8	-	-
	<i>nacad</i>	-	-	2	-	-
	<i>pxn1</i>	-	-	1	-	-
	<i>rasip1</i>	13	-	13	-	-
	<i>slc2a3</i>	15	-	15	-	-
	<i>steap4</i>	-	-	-	26	-
	<i>tbrg4</i>	-	-	2	-	-
<i>them4</i>	-	-	5	-	-	
<i>tnc</i>	-	-	1	-	-	
<i>twist1</i>	-	-	-	-	1	

	<i>zhx2</i>	5	-	6	-	-
	<i>znf628</i>	5	-	6	-	-
	Unannotated Regions	29	68	93	64	-
<b>Jaw closing In-Lever*</b>	<i>galr2</i>	-	-	-	2	-
<b>Orbit Diameter†</b>						
<b>Anterior Body Depth†</b>	<i>map2k6</i>	-	-	-	3	-
	<i>atp8a2</i>	92	-	92	-	-
	<i>cd226</i>	6	-	6	-	1
	<i>cdk8</i>	-	-	1	-	-
	<i>cmb1</i>	-	-	4	-	7
	<i>crispld1</i>	-	-	7	-	-
	<i>dok6</i>	-	-	50	-	-
	<i>fbxl7</i>	-	-	6	-	-
<b>Dentigerous Arm Depth*</b>	<i>hnf4g</i>	-	-	1	-	-
<b>Adductor Mandibulae</b>	<i>med1</i>	-	-	26	-	-
<b>Masst*</b>	<i>mtrr</i>	-	-	2	-	-
<b>Palatine Height†</b>	<i>ncoa2</i>	7	-	-	4	-
<b>Suspensorium Length†</b>	<i>prlh</i>	-	-	12	6	-
	<i>rnf6</i>	-	-	4	-	-
	<i>shisa2</i>	18	-	38	-	-
	<i>slc51a</i>	-	-	22	-	7
	<i>spice1</i>	4	-	2	-	-
	<i>ube2w</i>	-	48	-	-	-
	<i>zfhx4</i>	-	-	-	-	1
	Unannotated Regions	34	34	131	3	1

**Figure 1** A) Representative photographs of F2 intercross cleared and double-stained specimen used for skeletal morphometrics. Points represent landmarks used to measure linear distances between skeletal traits. B) Table containing the two landmarks that correspond to each trait.

A)



B)

Head			Body		
Point 1	Point 2	Trait	Point 1	Point 2	Trait
1	2	Lower Jaw Length	20	21	Premaxilla to Pelvic Girdle
2	3	Jaw closing In-Lever	20	31	Standard Length
2	4	Jaw Opening In-Lever	22	23	Cranium to Dorsal Fin
2	11	Palatine Height	23	24	Dorsal Fin Width
2	18	Suspensorium Length	23	25	Dorsal Fin Height
5	8	Dentigerous Arm Width	23	26	Anterior Body Depth
6	11	Maxilla Length	24	27	Posterior Body Depth
7	5	Dentigerous Arm Base	24	30	Caudal Peduncle Length
8	9	Dentigerous Arm Depth	26	27	Anal Fin Width
9	10	Ascending Process Length	27	28	Anal Fin Height
11	13	Maxillary Head Height	29	30	Caudal Peduncle Height
11	14	Ectopterygoid	For the Crescent Pond individuals, we recorded sex and the mass of the adductor mandibulae muscle before clearing and staining each specimen.		
12	13	Maxillary Head Protrusion			
12	19	Nasal Tissue Protrusion			
14	15	Orbit Diameter			
15	16	Cranial Height			
16	18	Head Depth			
17	18	Pelvic Girdle Length			

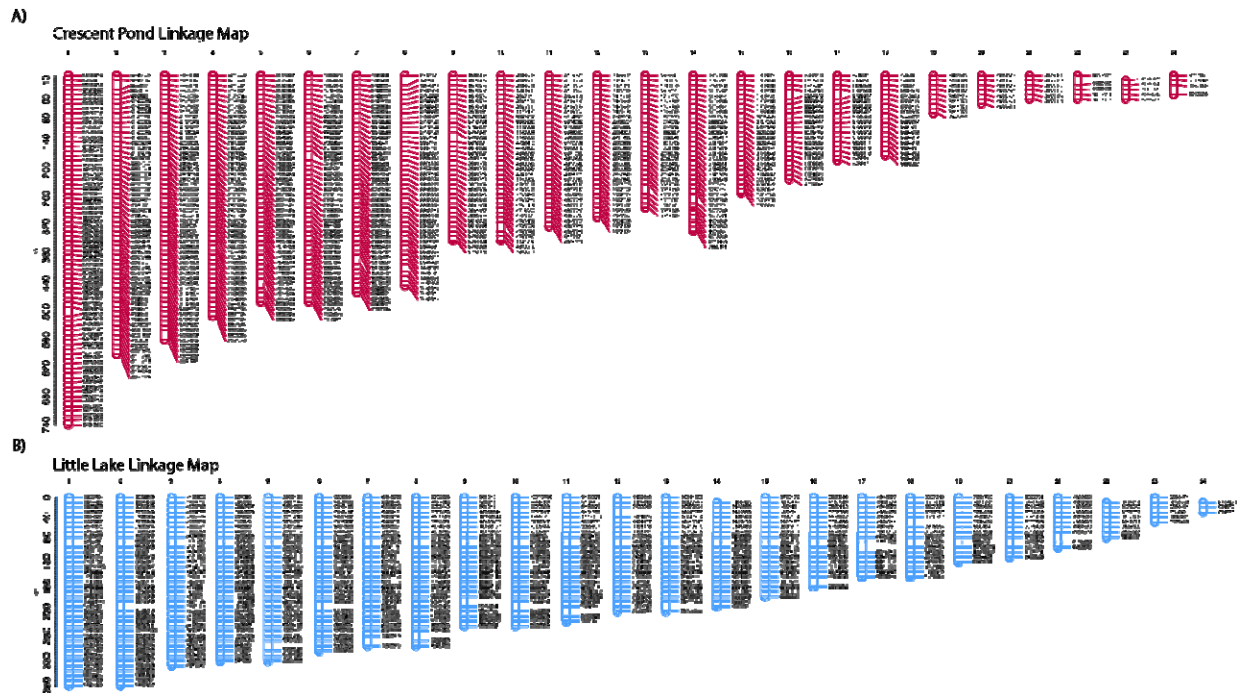


**Figure 2** Linkage maps for A) Crescent Pond and B) Little Lake crosses. The Crescent Pond linkage map was estimated from 743 markers and the Little Lake linkage map was estimated from 540 markers. Both maps were generated from crosses between a scale-eater (*C. desquamator*) and snail-eater (*C. brontotheroides*) from the respective lakes.

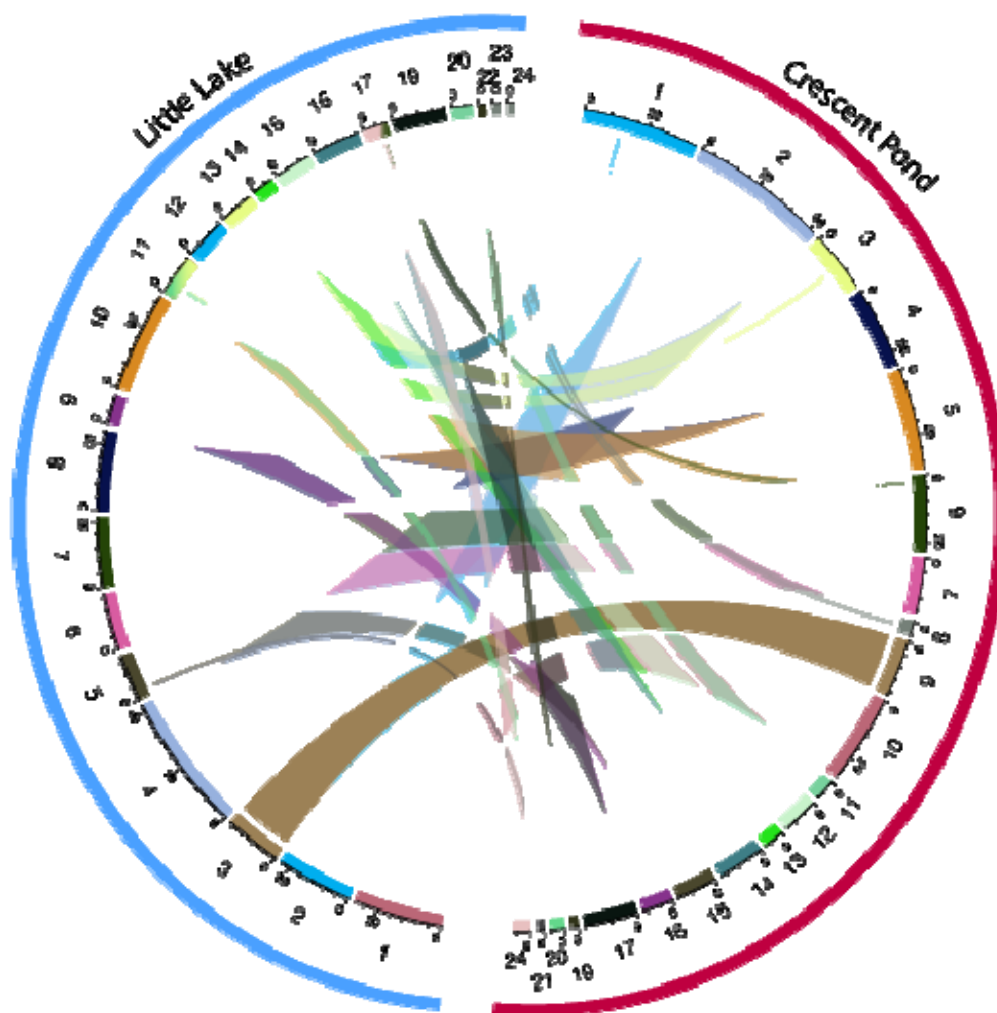


**Figure 3** Circos plot depicting the relationship between the Crescent Pond (red) and Little Lake linkage maps (blue), which share 324 markers within 10 kbp of one another. Numbers surrounding each semi-circle represent linkage group numbers in each lake. Markers that are shared across lakes are connected via the colored lines.

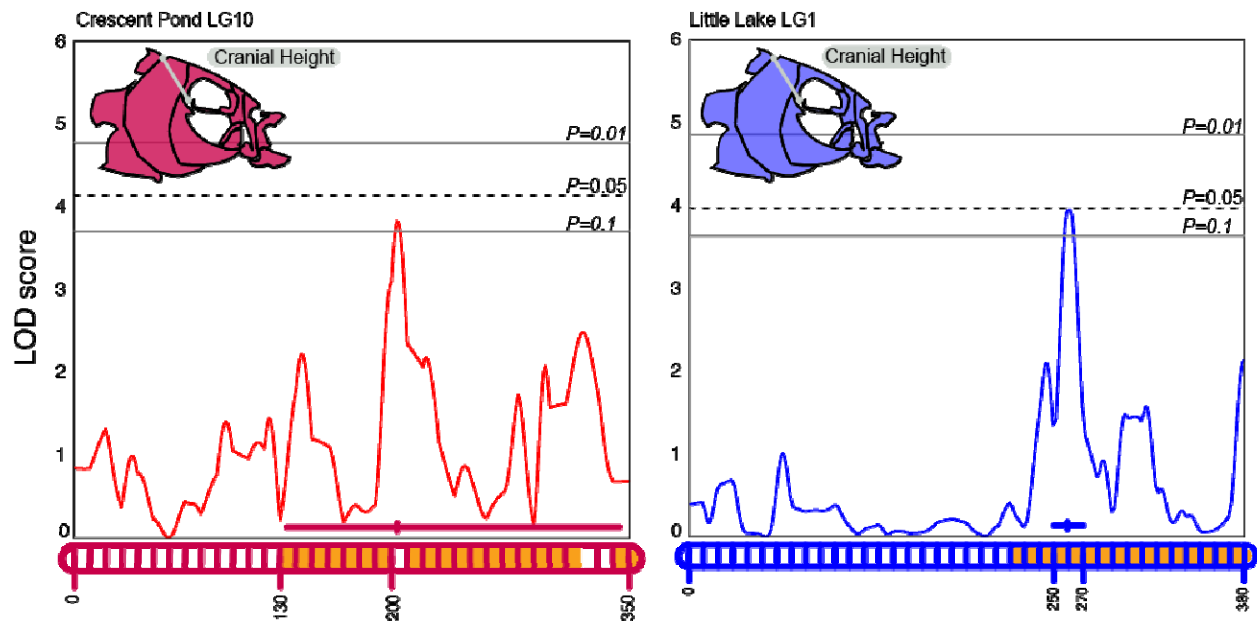


**Figure 4** LOD profile for cranial height in Crescent Pond (red) and Little Lake (blue) F2 hybrids. LOD profiles were estimated by a Haley-Knott regression and are plotted relative to the position along the implicated linkage group (LG 10 for Crescent Pond, LG 1 for Little Lake) which are represented along the X-axis. Genome wide significance levels of  $P = 0.1$ ,  $0.05$ , and  $0.01$  are shown by the grey horizontal lines. Linkage groups along the X-axis also show the position of maximum LOD along with 95% Bayesian credible intervals. The orange fill color within the linkage groups corresponds to overlapping regions of scaffold 33 between crosses.

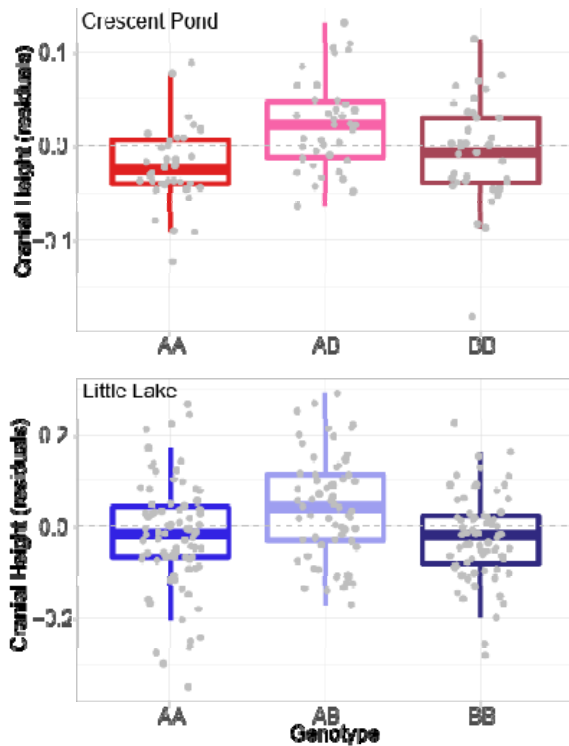


**Figure 5** Cranial height phenotypes (size-corrected residuals) for each genotype in Crescent Pond (red) and Little Lake (blue). Both lakes show that heterozygotes (AB) exhibit greater cranial heights than homozygous parental genotypes.